Robust Segmentation of 4D Cardiac MRI-tagged Images via Spatio-temporal Propagation

Zhen Qian[a], Xiaolei Huang[a], Dimitris Metaxas[a] and Leon Axel[b]

[a]Center for Computational Biomedicine, Imaging and Modeling (CBIM), Rutgers University, Piscataway, NJ, USA;
[b]Department of Radiology, New York University, New York, NY, USA

ABSTRACT

In this paper we present a robust method for segmenting and tracking cardiac contours and tags in 4D cardiac MRI tagged images via spatio-temporal propagation. Our method is based on two main techniques: the Metamorphs Segmentation for robust boundary estimation, and the tunable Gabor filter bank for tagging lines enhancement, removal and myocardium tracking. We have developed a prototype system based on the integration of these two techniques, and achieved efficient, robust segmentation and tracking with minimal human interaction.

Keywords: Tagged MRI, Metamorphs segmentation, Gabor filter bank, Tracking

1. INTRODUCTION

Cardiovascular diseases are the main cause of death in the western countries. Many heart diseases, such as ischemia and RV hypertrophy are thought to correlate strongly to the shape and motion of the heart. Tagged cardiac magnetic resonance imaging is a well-known technique for non-invasively visualizing the detailed myocardium motion and deformation. It has the potential of early diagnosis and analysis of these cardiovascular diseases. This technique generates a set of equally spaced parallel tagging plains within the myocardium as temporary markers at end-diastole by spatial modulation of magnetization. Imaging planes are perpendicular to the tagging planes, so that the tags appear as parallel dark stripes in MR images and deform with the underlying myocardium during the cardiac cycle *in vivo*, which gives motion information of the myocardium normal to the tagging stripes. Some example images can be seen from [Fig. (1)].

A set of spatio-temporal(4D) tagged MRI images of the heart provides qualitative and quantitative information about the morphology, kinematic function and material properties of the heart. However, before this technique being used in the routine clinical evaluation, we need to solve the following image analysis tasks:

1. Extraction and tracking of the heart wall boundaries and tags.
2. LV-RV shape and motion analysis.
3. Myocardium strain analysis.
4. Modeling the intra-cavity flow, etc.

It has been noted by several researchers that the rate-limiting step which prevents tagged MR from clinical use is the robust extraction and tracking of the contours and tags. There have been a vast research efforts on the automated contour segmentation, however, it still remains a difficult task due to the common presence of cluttered objects, complex object textures, image noise, intensity inhomogeneity, and especially the complexities added by the tagging lines.

In this paper, to address the difficulty added by tagging lines, before the segmentation process, a tunable Gabor filter bank technique is first applied to remove the tagging lines and enhance the tag-patterned region.[1] This method is based on the idea that by tuning the phase angle of the Gabor filter we are able to fill in the areas between tagging lines. Because after the initial tagging modulation, the tag patterns in the blood are flushed

Further author information: (Send correspondence to Z. Qian)
Z. Qian.: E-mail: zqian@eden.rutgers.edu, Telephone: 1 732 445 2795

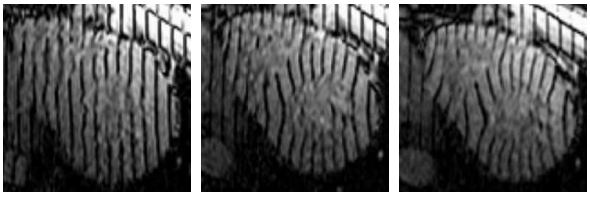

Figure 1. Three images from a time sequence of the cardiac tagged MR images in the short axis.

out very soon, this de-tagging technique actually enhances the blood-myocardium contrast and facilitates the following myocardium segmentation.

Our segmentation framework is based on a newly proposed deformable model, which we call "Metamorphs".[2] The key advantage of the Metamorph models is that it integrates both shape and interior texture and its dynamics are derived coherently from both boundary and region information in a common variational framework. These properties of Metamorphs make it more robust to image noise and artifacts than traditional shape-only deformable models.

A full set of conventional spatio-temporal(4D) tagged MRI consists of more than one thousand images. Segmenting every image individually is a time-consuming process that is not clinically feasible. We propose a new myocardium tracking technique which enables temporal propagation of the heart wall boundaries over the heart beat cycle. Through this propagation, we only need to do myocardium segmentation at one time, then it will be propagated both spatially and temporally to segment the whole set efficiently. This method is based on implementing a tunable Gabor filter bank to observe the deformations of the tagging lines over time.[3] This is possible because we can approximate the displacements (or deformations) of the tagging patterns by estimating the changes in parameter values of the Gabor filters that maximize the Gabor response over time. The motion of the tagging lines indicates the underlying motion of the myocardium, and therefore, the motion of the heart wall boundaries. Spatial propagation of the heart wall boundaries is more difficult due to the complex heart geometry and the topological changes of the boundaries at different positions of the heart. Our solution is segmenting a few key slices first, which represent the topologies of the rest of the slices. Then we let the key frames propagate to the remaining slices.

The remainder of this paper is organized as follows: in Section 2, we briefly introduce the Metamorphs segmentation on model shape, texture, deformations and dynamics. In Section 3, we present the theory of the tunable Gabor filter bank and its applications in tag removal and myocardium tracking. We introduce the integration of the Metamorphs and Gabor filter bank methods in Section 4 with our phototype system and some experimental results as this paper's conclusion.

2. THE METAMORPH DEFORMABLE MODEL FOR TAGGED MR IMAGE SEGMENTATION

2.1. The Model's Shape Representation

In our framework, the shape of an evolving model is implicitly embedded as the zero level set of a higher dimensional distance function using the Euclidean distance transform.[4] Let $\Phi : \Omega \rightarrow R^+$ be a Lipschitz function that refers to the distance transform for the model shape $\mathcal{M}$. The shape defines a partition of the domain: the region that is enclosed by $\mathcal{M}$, $[\mathcal{R}_\mathcal{M}]$, the background $[\Omega - \mathcal{R}_\mathcal{M}]$, and on the model, $[\partial\mathcal{R}_\mathcal{M}]$. Given these definitions the following implicit shape representation is considered:

$$\Phi_\mathcal{M}(\mathbf{x}) = \begin{cases} 0, & \mathbf{x} \in \partial\mathcal{R}_\mathcal{M} \\ +ED(\mathbf{x},\mathcal{M}) > 0, & \mathbf{x} \in \mathcal{R}_\mathcal{M} \\ -ED(\mathbf{x},\mathcal{M}) < 0, & \mathbf{x} \in [\Omega - \mathcal{R}_\mathcal{M}] \end{cases}$$

where $ED(\mathbf{x},\mathcal{M})$ refers to the min Euclidean distance between the image pixel location $\mathbf{x} = (x, y)$ and the model $\mathcal{M}$.

Such treatment makes the model shape representation an "image", which greatly facilitates the integration of boundary and region information. It also provides a feature space in which objective functions that are optimized using a gradient descent method can be conveniently used, since the gradient of the distance function consists of continuous unit vectors in the normal direction of the shape.

2.2. The Model's Deformations

The model deformations are efficiently parameterized using a space warping technique, the cubic B-spline based Free Form Deformations (FFD).[5,6] The essence of FFD is to deform an object by manipulating a regular control lattice F overlaid on its volumetric embedding space. In this paper, we consider an Incremental Free Form Deformations (IFFD) formulation using the cubic B-spline basis.[7]

Let us consider a regular lattice of control points

$$F_{m,n} = (F^x_{m,n}, F^y_{m,n});\ m = 1, ..., M, \quad n = 1, ..., N$$

overlaid to a region $\Gamma_c = \{\mathbf{x}\} = \{(x, y)|1 \le x \le X, 1 \le y \le Y\}$ in the embedding space that encloses the model in its object-centered coordinate system. Let us denote the initial configuration of the control lattice as F^0, and the deforming control lattice as $F = F^0 + \delta F$. Under these assumptions, the incremental FFD parameters, which are also the deformation parameters for the model, are the deformations of the control points in both directions (x, y):

$$\mathbf{q} = \{(\delta F^x_{m,n}, \delta F^y_{m,n})\};\ (m, n) \in [1, M] \times [1, N]$$

The deformed position of a pixel $\mathbf{x} = (x, y)$ given the deformation of the control lattice from F^0 to F, is defined in terms of a tensor product of Cubic B-spline polynomials:

$$D(\mathbf{q}; \mathbf{x}) = \mathbf{x} + \delta D(\mathbf{q}; \mathbf{x}) = \sum_{k=0}^{3}\sum_{l=0}^{3} B_k(u)B_l(v) (F^0_{i+k,j+l} + \delta F_{i+k,j+l}) \tag{1}$$

where $i = \lfloor \frac{x}{X} \cdot (M-1) \rfloor + 1,\ j = \lfloor \frac{y}{Y} \cdot (N-1) \rfloor + 1;\ \delta F_{i+l,j+l},\ (k, l) \in [0, 3] \times [0, 3]$ are the deformations of pixel $\mathbf{x}$'s (sixteen) adjacent control points; $B_k(u)$ is the k^{th} basis function of a Cubic B-spine, with $u = \frac{x}{X} \cdot (M-1) - \lfloor \frac{x}{X} \cdot (M-1) \rfloor$, and $B_l(v)$ is similarly defined. Also based on the linear precision property of B-splines, we have $\delta D(\mathbf{q}; \mathbf{x}) = \sum_{k=0}^{3}\sum_{l=0}^{3} B_k(u)B_l(v)\delta F_{i+k,j+l}$ is the incremental deformation for pixel $\mathbf{x}$.

2.3. The Model's Texture

The interior intensity statistics of the models are captured using nonparametric kernel-based approximations, which can represent complex multi-modal distributions.

Suppose the model is placed on an image I, the image region bounded by current model $\Phi_{\mathcal{M}}$ is $\mathcal{R}_{\mathcal{M}}$, then the probability of a pixel's intensity value i being consistent with the model interior intensity can be derived using a Gaussian kernel as:

$$\mathbf{P}(i|\Phi_{\mathcal{M}}) = \frac{1}{V(\mathcal{R}_{\mathcal{M}})} \iint_{\mathcal{R}_{\mathcal{M}}} \frac{1}{\sqrt{2\pi}\sigma} e^{\frac{-(i-I(\mathbf{y}))^2}{2\sigma^2}} d\mathbf{y} \tag{2}$$

where $V(\mathcal{R}_{\mathcal{M}})$ denotes the volume of $\mathcal{R}_{\mathcal{M}}$, and σ is a constant specifying the width of the gaussian kernel.

Using this nonparametric approximation, the intensity distribution of the model interior gets updated automatically while the model deforms.

2.4. The Metamorph Dynamics

When finding object boundaries in images, the dynamics of the Metamorph models are derived from an energy functional consisting of both edge/boundary energy terms and intensity/region energy terms. The overall energy functional E consists of two shape data terms – an interior term E_{S_i} and a boundary term E_{S_b}, and two intensity terms – a "Region Of Interest" (ROI) term E_{I_r} and a Maximum Likelihood term E_{I_m}:

$$E = (E_{S_i} + aE_{S_b}) + k(E_{I_r} + bE_{I_m}) \tag{3}$$

where k is a constant factor balancing the contribution from the shape vs. intensity terms, a is a factor balancing the two shape terms, and b is a factor balancing the two intensity terms.

In our formulation, both shape data terms and intensity data terms are differentiable with respect to the model deformation parameters $\mathbf{q}$, thus a unified gradient-descent based parameter updating scheme can be derived using both boundary and region information. One can derive the following evolution equation for each element $\mathbf{q}_i$ in the model deformation parameters $\mathbf{q}$:

$$\frac{\partial E}{\partial \mathbf{q}_i} = \big(\frac{\partial E_{S_i}}{\partial \mathbf{q}_i} + a\frac{\partial E_{S_b}}{\partial \mathbf{q}_i}\big) + k\big(\frac{\partial E_{I_r}}{\partial \mathbf{q}_i} + b\frac{\partial E_{I_m}}{\partial \mathbf{q}_i}\big) \tag{4}$$

The detailed definitions of all four energy terms based on image data and the gradient derivation for each term can be found in.[2]

2.5. The Model Fitting Algorithm and Tagged MR Image Segmentation Results

During boundary finding, the overall model fitting algorithm consists of the following steps:

1. Initialize the deformation parameters $\mathbf{q}$ to be $\mathbf{q}^0$, which indicates no deformation.
2. Compute $\frac{\partial E}{\partial \mathbf{q}_i}$ for each element $\mathbf{q}_i$ in the deformation parameters $\mathbf{q}$.
3. Update the parameters $\mathbf{q}_i' = \mathbf{q}_i - \lambda \cdot \frac{\partial E}{\partial \mathbf{q}_i}$.
4. Using the new parameters, compute the new model $\mathcal{M}' = D(\mathbf{q}'; \mathcal{M})$.
5. Update the model. Let $\mathcal{M} = \mathcal{M}'$, re-compute the implicit representation of the model $\Phi_{\mathcal{M}}$, and the new partitions of the image domain by the new model: $[\mathcal{R}_{\mathcal{M}}]$, $[\Omega - \mathcal{R}_{\mathcal{M}}]$, and $[\partial\mathcal{R}_{\mathcal{M}}]$. Also re-initialize a regular FFD control lattice to cover the new model, and update the new model interior intensity statistics.
6. Repeat steps 1-5 until convergence.

In the algorithm, after each iteration, both shape and interior intensity statistics of the model get updated based on the model dynamics, and deformation parameters get re-initialized for the new model. This allows continuous, both large-scale and small-scale deformations for the model to converge to the energy minimum.

We used Metamorph models to segment heart boundaries in tagged MR images, both on original images with tags and on de-tagged images that have tags removed by gabor filtering. In [Fig. (2)], we show the Left Ventricle, Right Ventricle, and Epicardium segmentation using Metamorphs on de-tagged MR images. By having the tagging lines removed using gabor filtering, a Metamorph model can get close to the heart wall boundary more rapidly. Then the model can be further refined on the original tagged image.

The Metamorph model evolution is computationally efficient, due to our use of the nonparametric texture representation and FFD parameterization of the model deformations. For all the examples shown, the segmentation process takes less than $200ms$ to converge on a 2Ghz PC station.

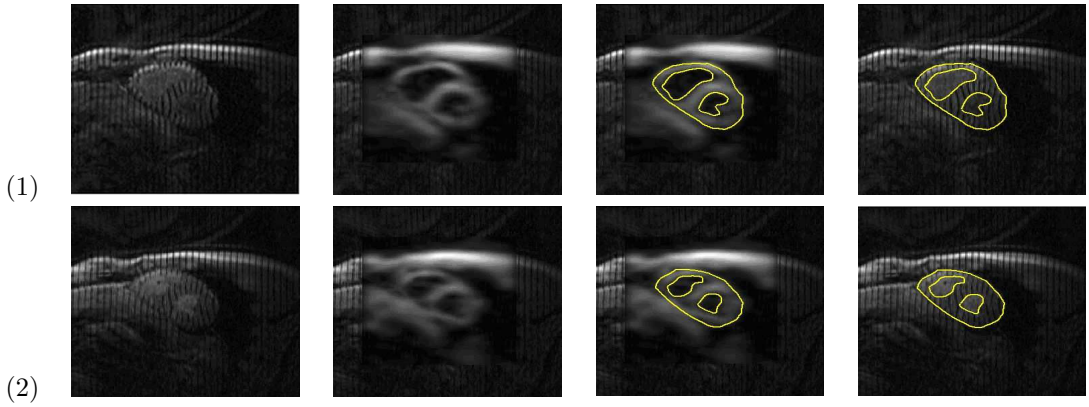

Figure 2. Metamorphs segmentation on de-tagged images. (1) segmentation at time 7, slice position 7. (2) segmentation at time 7, slice position 10. (a) original image. (b) image with tags removed by gabor filtering. (c) cardiac contours segmented by Metamorphs on detagged image. (d) contours projected on the original image.

3. THE GABOR FILTER BANK TECHNIQUE FOR TAGGED MRI ANALYSIS

3.1. Basic Definitions

Gabor filters have been widely used in image processing applications, such as texture segmentation[8–10] and edge detection.[11] A main advantage of Gabor filters is that they always achieve the minimum space-bandwidth product which is specified in the uncertainty principle due to their Gaussian envelopes .

The 2D Gabor filter was first introduced by Daugman.[12] It is basically a 2D Gaussian multiplied by a complex 2D sinusoid,[8] as shown below:

$$h(x,y) = g(x',y') \cdot s(x,y) \tag{5}$$

where $g(x',y')$ is a 2D Gaussian, and $s(x,y)$ is a complex 2D sinusoid function, i.e.,

$$g(x',y') = \frac{1}{2\pi\sigma_{x'}\sigma_{y'}} \exp\{-\frac{1}{2}[(\frac{x'}{\sigma_{x'}})^2 + (\frac{y'}{\sigma_{y'}})^2]\} \tag{6}$$

$$s(x,y) = \exp[-j2\pi(Ux + Vy)] \tag{7}$$

In (6): $x' = xcos\theta + ysin\theta, y' = -xsin\theta + ycos\theta$ are the spatial coordinates which are rotated by an angle θ, and σ_x, σ_y gives the approximate spatial extent of the 2D Gaussian. The 2D Gaussian envelope need not be symmetric, where σ_x and σ_y are not equal. In our case, this asymmetry fits the tag pattern better: in the orientation that is perpendicular to the tagging lines, the tag pattern is stronger than in the orientation that is parallel to the tagging lines. So we experimentally set the Gaussian envelope as an ellipsoid whose long axis is 4 times as long as the short axis. We define the σ's of the 2D Gaussian as in (8) and (9):

$$\sigma_x = \frac{1}{\sqrt{(U^2 + V^2)}} \tag{8}$$

$$\sigma_y = \frac{1}{\sqrt{(U^2 + V^2)}} \cdot \frac{1}{4} \tag{9}$$

In (7), (U, V) are the 2D frequencies of the complex sinusoid, and its orientation in frequency domain is given by:

$$\phi = \arctan(V/U) \tag{10}$$

At time 1 of the tagged MR imaging process, when the tagging lines are initially straight and equally spaced, in the spectral domain of the input tagged MR image, there exist several isolated harmonic peaks representing its frequency characteristics. And the first harmonic peak represents the main patterns of the image, which are the un-deformed tagging lines. We set the parameters (U, V) of the Gabor filter to capture the un-deformed tag pattern by automatically finding the coordinates of the image's first harmonic peaks in the spectral domain.

Because the input images are taken during a heart beat cycle, the tagging lines move along with the underlying myocardium, and the spacings and orientations of them change accordingly. These changes in the spatial domain lead to corresponding changes in the frequency domain. The new U' and V' are tuned as follows:

$$U' = \Re\{(U + i \cdot V) \cdot m \cdot \exp(i \cdot \Delta\phi + \omega)\} \tag{11}$$

$$V' = \Im\{(U + i \cdot V) \cdot m \cdot \exp(i \cdot \Delta\phi + \omega)\} \tag{12}$$

Where m, $\Delta\phi$, and ω are the magnitude, the angle and the phase modulation respectively in the frequency domain. Thus backwardly we may modulate m corresponding to the changes of tag spacing, and modulate $\Delta\phi$ corresponding to the changes of the tag lines' orientations. Phase angle ω modulation represents the relative position of the current pixel with respect to the nearby tagging line.

The orientation of the Gaussian envelope θ need not be the same as the orientation of the sinusoid. But for the purpose of normalization, we set these two angles with the same value, thus the sinusoid is always perpendicular to the long axis of the Gaussian envelope. This is essential if we don't do normalization later but still be able to achieve decent results.

3.2. Tagging Lines Enhancement and Removal

We modify the parameters m, $\Delta\phi$, and ω of the un-tuned Gabor filter to fit the deformed tag patterns. The original un-tuned Gabor filter and the modified Gabor filters make up a tunable Gabor filter bank.

By convolving the input tagged MRI with an m and $\Delta\phi$ tunable Gabor filter bank, the pixels in any variously deformed tagging lines, which have different tag-spacings and orientations, are enhanced and extracted out. The final extraction results are combination of the filtering results of each Gabor filter in the filter bank.[13] (As shown in [Fig. (3)] Practically, the convolution step is computed as a production in the Fourier domain for faster implementation:

$$I * g = \mathcal{F}^{-1}\{\mathcal{F}\{I\} \cdot \mathcal{F}\{g\}\} \tag{13}$$

Figure 3. The extraction results of the MR images in [Fig. (1)]. The myocardium contours are drawn manually for better radiabilities.

The modulation of phase angle ω represents the relative position of the current pixel with respect to the nearby tagging line. Tuning ω makes the enhanced region shift away from the tagging lines, therefore the tag enhancing operation also occurs at pixels between or near the tagging lines. Thus by tuning all the three parameters, m, $\Delta\phi$, and ω, of the Gabor filter, we get high responses from Gabor filtering not only in those variously deformed tagging lines, but also in the regions between or near these tagging lines. By combining the enhancing results from each filter in the "*all-three-parameter-tunable*" Gabor filter bank, we can fill in the areas that are between or near the deformed tagging lines, i.e., the tagging lines are removed and the tag-patterned areas are enhanced.

$$I_{tag\_removed} = \int_m \int_{\Delta\phi} \int_{\omega=-\pi}^{\pi} I * g(\omega) dm d\Delta\phi d\omega \tag{14}$$

Because after the initial tagging modulation, the tag patterns in the blood are flushed out very soon, this tag removal method can enhance the blood-myocardium contrast and facilitate myocardium segmentation. As shown in [Fig. (2)], the de-tagged images in mid-systolic phase make the boundary segmentation tasks easier.

3.3. Myocardium Tracking

At each pixel in the input image, we apply the tunable Gabor filter bank and find out a set of optimal filter parameters, m, $\Delta\phi$, and ω, that maximize the Gabor filter response. The optimal parameter values at each pixel make up of three parameter maps that tell the region properties around the certain pixel. Figure 4 are the parameter maps that consist of those optimal parameter values. The tagging lines' spacing, orientations and the relative positions of each pixel are clearly illustrated. At the same time, a threshold is applied based on the value of the maximum response of the Gabor filter bank. When there is no tagging lines in a certain area, the Gabor response becomes very weak and thus below a certain threshold, then this area will be wiped out and we won't consider it. (As the gray area shown in [Fig. (4)].)

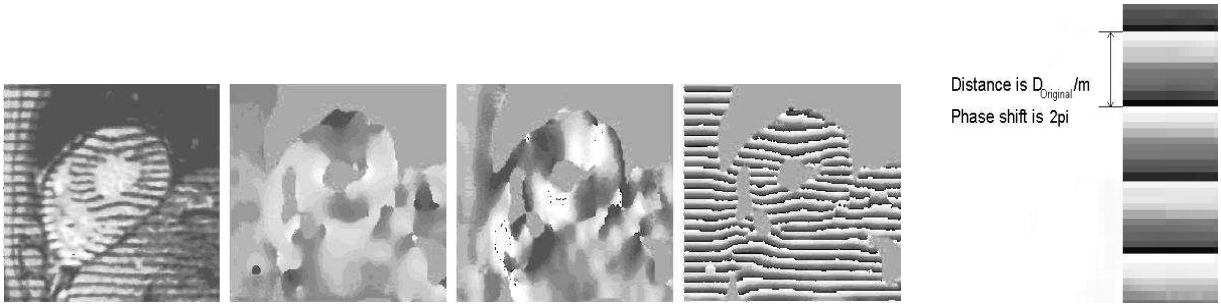

Figure 4. The first image is the original input MR image. The second one is the spacing m map. The bright color indicates the spacing between tagging lines are smaller, and the dark color indicates the spacing bigger. The third image is the orientation $\Delta\phi$ map. The bright color means the orientation of the tagging lines is from lower left to upper right; the dark color means the orientation is from lower right to upper left. The fourth image is the phase ω map. The color varying from dark to bright means the phase angles vary from $-\pi$ to $+\pi$. The gray areas in the maps mean the parameters are not changed or there is no tagging lines. The last figure illustrates the relationship between tag spacing the phase shift.

From the m map and the ω map, we can learn the tissue's relative distance with respect to the nearby tagging lines, i.e., at a certain pixel, the distance between this pixel and the nearby tagging line is determined by:

$$D = D_{original} \cdot \omega / (2\pi \cdot m) \tag{15}$$

Where $D_{original}$ is the original spacing between two undeformed tagging lines. If the deformation of a certain material point in 2 intermediate time sequent MRI is not bigger than a half of the spacing between two nearby tagging lines, which is true in most of our tagging MRI images because of the high imaging speed and the relatively slow heart deformation, the change of the ω maps coupled with the m maps can approximately tell the displacement of the underlying tissue by:

$$\begin{aligned} \Delta D &= D_{original} \cdot \Delta\omega / (2\pi \cdot m) \\ &= D_{x\_original} \cdot \Delta\vec{\omega}_x / (2\pi \cdot m_x) + D_{y\_original} \cdot \Delta\vec{\omega}_y / (2\pi \cdot m_y) \end{aligned} \tag{16}$$

For conventional short axis(SA) tagged MRI sequences, we have two sets of data whose tagging lines are initially perpendicular to each other. Thus we can use (16) to calculate the deformations in two different orientations at each pixel in the time sequence. When we combined the horizontal and vertical deformations from the two data sets, we get the deformation of the myocardium.

According to the deformations of the tagging lines, the modulation range of the Gabor filter bank parameters are empirically set by:

$$\begin{aligned} m &\in [0.85, 1.3] \\ \Delta\phi &\in [-\pi/12, \pi/12] \\ \omega &\in [-\pi, \pi] \end{aligned} \tag{17}$$

In [Fig. (5)] we show a set of myocardium tracking results from time 1 to time 10. We impose a 2D grid mesh onto the myocardium area and let it deform with the underlying tissue. There are some irregular deformations in some local regions because the tracking depends on the tag texture pattern alone, and MR images usually have high level noise. However the overall movement matches the underlying tissue motion properly. And after smoothing, it is good enough for further boundary tracking tasks.

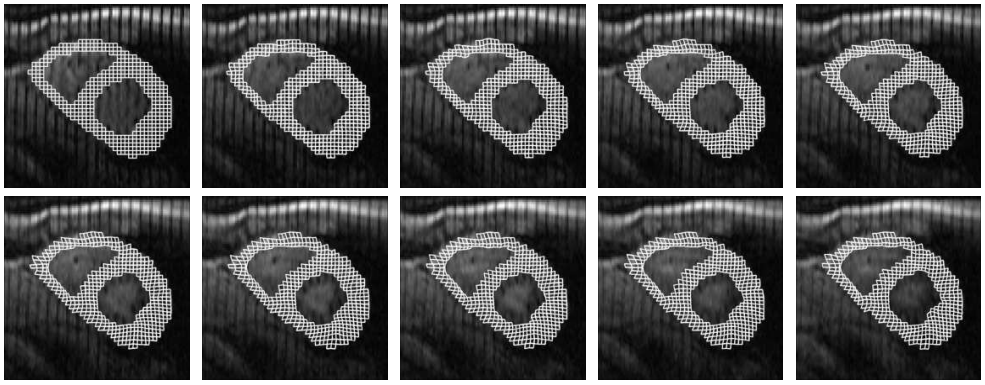

Figure 5. A mesh is imposed on the myocardium area and deforms along time. We find the mesh contracts properly as the underlying heart muscle contracts. In some local regions, the mesh deformation results look not very accurate. However after smoothing, this tracking results are good enough for the following boundary tracking.

4. INTEGRATION AND THE PROTOTYPE SYSTEM

We integrate the above two major techniques, the tunable Gabor filter bank and the Metamorphs segmentation, to construct our 4D spatio-temporal integrated MR analysis system. By using the two techniques in a complementary manner, exploiting specific domain knowledge about the heart anatomy and temporal characteristics of the tagged MR images, we can achieve efficient, robust segmentation with minimal user interaction. The algorithm consists of the following main steps. (The illustration of the spatio-temporal propagation can be found in [Fig. (6)].)

1. Tag removal for images at the mid-systolic phase. Given a 4D spatio-temporal tagged MR image dataset of the heart, we start by filtering using a tunable Gabor filter bank on images of a 3D volume that corresponds to a particular time in the middle of the systolic phase, which we term *'center time'*. For a typical dataset in which the systolic phase is divided into 13 time intervals, we apply the Gabor filtering on images at time 7, when tag patterns in the endocardium are flushed out by blood but tag lines in the myocardium are clearly visible.

2. Metamorphs segmentation using the de-tagged images. Given the de-tagged Gabor response images at time 7, we use Metamorphs to segment the cardiac contours including the epicardium, the LV and RV endocardium. Since the formulation of Metamorphs naturally integrates both shape and interior texture, and the model deformations are derived from both boundary and region information, the Metamorph models can be initialized far-away from the object boundary and efficiently converge to an optimal solution. For each image, we first segment the LV and RV endocardium. To do this, the user initializes a circular model by clicking one point (the seed point) inside the object of interest, then the surrounding region intensity statistics and the gradient information automatically drive the model to converge to the endocardium boundaries. We then automatically initialize a metamophs model for the epicardial contour by merging the endocardial contours and expanding the

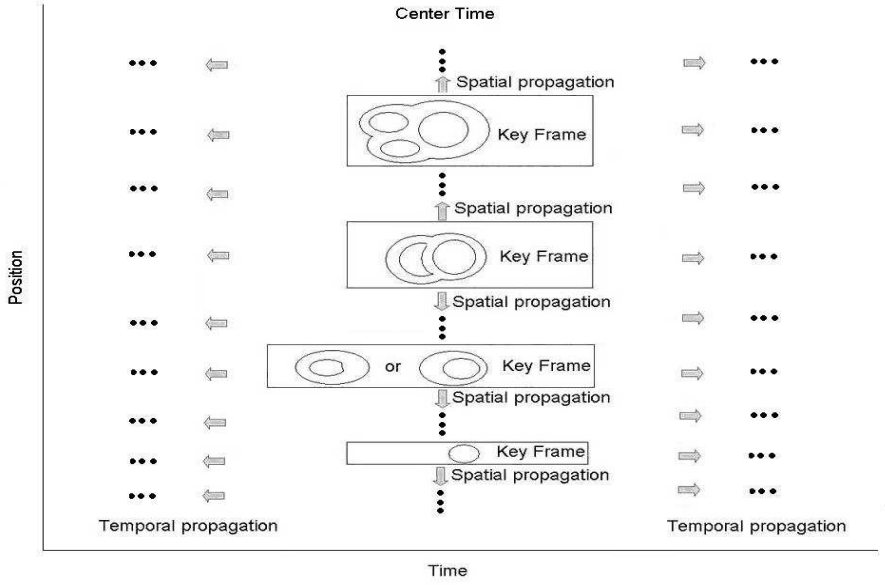

Figure 6. The framework of our automated segmentation in 4D spatio-temporal MRI-tagged images. We start at a center time when the tag lines are flushed away in the blood area while they remain clear in the myocardium. Boundary segmentation is done in several key frames on the de-tagged images before the boundary contours are spatially propagated to the other positions. Then at each position, the boundaries are temporally propagated to other times.

interior volume according to myocardium thickness statistics. The model is then allowed to evolve and converge to the epicardium boundary.

3. Spatial propagation at the mid-systolic center time. At the mid-systolic phase, we do the segmentation at several key frames which represent the topologies of the rest of the frames, then let the segmented contours propagate to their nearby frames. In short axis cardiac MR images, from the apex to the base, the topology of the boundaries goes through the following variations: 1. one epicardium; 2. one epicardium and one LV endocardium (in some cases of the RV hypertrophy patients, one epicardium and one RV endocardium are also possible); 3. one epicardium, one LV endocardium and one RV endocardium; 4. one epicardium, one LV endocardium and two RV endocardium. The key frames consist of one center frame of the third topology and three transition frames. This spatial propagation actually provides a quick initialization method (rather than manually clicking the seed points as mentioned in step 2) for the rest of the non-key frames from the key frames.

4. Boundary tracking using tunable Gabor filters over time. Once we have segmented the cardiac contours at time 7, we keep tracking the motion of the myocardium and the segmented contours over time. This temporal propagation of the cardiac contours significantly reduces computation time, since it enables us to do supervised segmentation at only one time, then fully automated segmentation of the complete 4D dataset can be achieved. It also improves segmentation accuracy because we capture the overall trend in heart deformation more accurately by taking into account the temporal connection between segmented boundaries.

5. Boundary refinement using Metamorphs. In practice, we provide the option to further refine the boundaries using Metamorph deformable models, which are automatically initialized using the tracked contours. We also provide the manual correction option to doctors during the whole segmentation process to ensure satisfiable results.

6. Tagging lines tracking within the heart wall. Tagging lines are straight lines at time 0. They are equally spaced at an interval of $1/\sqrt{(U^2+V^2)}$. Starting from time 0, we keep tracking the tagging lines only *within the heart wall* from the results of the boundary segmentation and boundary tracking steps above. The tagging lines' model is basically a set of *Snakes* whose external forces are from the original intensity images and the tag-enhanced images.

The prototype of our 4D segmentation system is developed in a Matlab 6.5 GUI environment. The user need to load in the raw MRI data of the short axis and long axis volumes first ([Fig. (9-1a)]). Then the user is allowed to examine the whole data sets, which consist of two short axes and one long axis, and determine the slice index of the center time ([Fig. (9-1b,1c,2a)]). The tag removal step is done on the 3D volume at the center time ([Fig. (9-2b)]). Then the user has a option to determine the indices of the key frames and do Metamorphs segmentation on these key frames ([Fig. (9-2c,3a,3b,3c)]). The segmented contours are propagated spatially (optional) and then temporally ([Fig. (9-4a,4b)]). Practically the spatial propagation step is optional because for most clinical analysis one typical slice is enough unless a fully 4D model is required. Manual interaction is always available during the whole segmentation and propagation process to make corrections in time. Based on the boundary segmentation results, the user are able to track the tagging lines from time 1 [(Fig. (9-4c)]). The initialization and tracking of the tag tracking is totally automatic. However, manual corrections is also available. Figure 8 is a set of contour segmentation and tagging lines tracking results generated by this system.

5. CONCLUSION

Several novel aspects of our proposed integration contribute to the effective nature of our approach. First, we are the first to propose and evaluate the feasibility to use deformable shape and texture models on tag-removed images for segmenting cardiac objects. Second, we design our algorithm based on our belief that, to achieve robust and automated segmentation in 4-D, we have to use information from 4D. Hence the temporal tracking and spatial segmentation are tightly coupled in our approach. The deformable model based segmentation at a mid-systolic phase provides initialization for the tracking process, while the contour tracking returns close and reliable initialization for deformable model based segmentation at all other times. Third, the basis techniques we use, i.e. the tunable Gabor filter bank and deformable shape and texture models (MetaMorphs), are both cutting-edge techniques that have been recently developed and recognized by the research community. Applying these techniques to the difficult tagged-MR cardiac segmentation problem has posed new challenges to the techniques themselves and in turn supported their improvements. The integration of tunable Gabor filter bank and deformable shape and texture models has enabled us to develop a generic, efficient framework for segmenting 4D spatial-temporal tagged MR images. The software that resulted from this work requires minimal user interaction, and is robust and accurate enough for clinical evaluation.

ACKNOWLEDGMENTS

This work has been supported by the grants from NIH and NSF (NSF-ITR) to Dr. Dimitris Metaxas and Dr. Leon Axel.

REFERENCES

1. T. Manglik, L. Axel, W. Pai, D. Kim, P. Dugal, A. Montillo, and Z. Qian, "Use of bandpass gabor filters for enhancing blood-myocardium contrast and filling-in tags in tagged mr images," in *Proc of Int'l Society for Mag. Res. In Med.*, p. 1793, 2004.
2. X. Huang, D. Metaxas, and T. Chen, "Metamorphs: Deformable shape and texture models," in *IEEE Conf. on Computer Vision and Pattern Recognition*, **1**, pp. 496–503, 2004.
3. A. Montillo, L. Axel, and D. Metaxas, "Extracting tissue deformation using gabor filter banks," in *Proc of SPIE: Medical Imaging: Physiology, Function, and Structure from Medical Images*, **5369**, pp. 1–9, 2004.
4. S. Osher and J. Sethian, "Fronts propagating with curvature-dependent speed : Algorithms based on the Hamilton-Jacobi formulation," *Journal of Computational Physics* **79**, pp. 12–49, 1988.
5. T. W. Sederberg and S. R. Parry, "Free-form deformation of solid geometric models," in *Proceedings of the 13th Annual Conference on Computer Graphics*, pp. 151–160, 1986.
6. A. A. Amini, Y. Chen, M. Elayyadi, and P. Radeva, "Tag surface reconstruction and tracking of myocardial beads from SPAMM-MRI with parametric b-spline surfaces," *IEEE Transactions on Medical Imaging* **20**(2), pp. 94–103, 2001.
7. X. Huang, N. Paragios, and D. Metaxas, "Establishing local correspondences towards compact representations of anatomical structures," in *Proc. of Int'l Conf. on Medical Imaging Computing and Computer-Assisted Intervention, LNCS 2879*, pp. 926–934, 2003.
8. D. Dunn, W. E. Higgins, and J. Wakeley, "Texture segmentation using 2-d gabor elementary functions," *IEEE Trans. Pattern Anal. and Machine Intell* **16**, pp. 130–149, 1994.

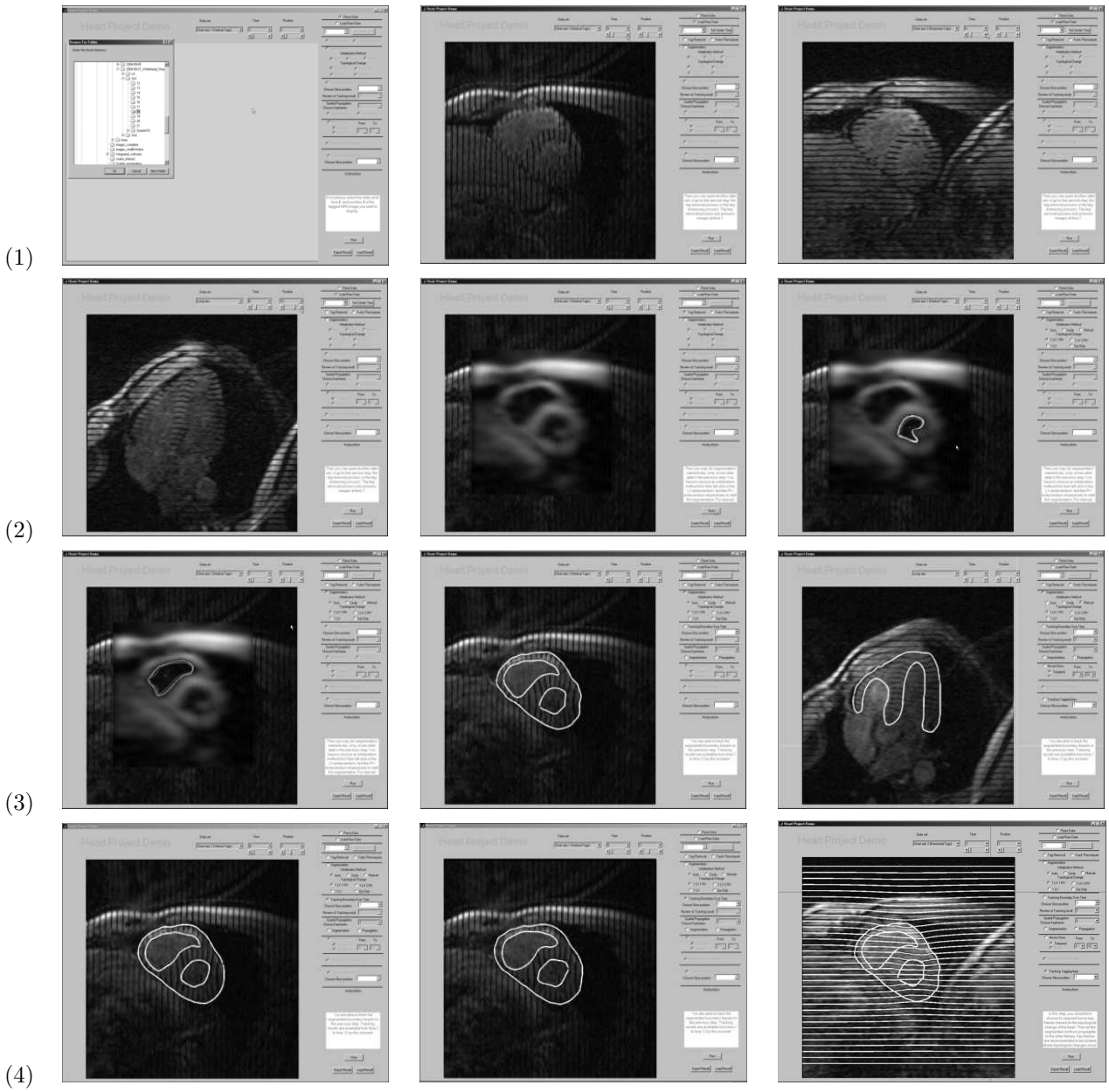

Figure 7. Screen snapshots of our segmentation and tracking system. (1a) read in the SA and LA volumes. (1b,1c,2a) examine the data sets. (2b) de-tagged image at the center time. (2c,3a) Metamorphs segmentation based on de-tagged images. (3b,3c) segmentation results. The papillary muscle is excluded from the myocardium by manual interaction. (4a,4b) temporal propagation. (4c) tagging lines tracking.

9. T. P. Weldon, W. E. Higgins, and D. F. Dunn, "Efficient gabor filter design for texture segmentation," *Journal of Pattern Recognition* **29**(12), pp. 2005–2016, 1996.
10. T. P. Weldon and W. E. Higgins, "An algorithm for designing multiple gabor filters for segmenting multitextured images," in *IEEE Int'l Conf. on Image Processing*, **3**, pp. 333–337, 1998.
11. R. Mehrotra, K. R. Namuduri, and N. Ranganathan, "Gabor filter-based edge detection," *Journal of Pattern Recognition* **25**, pp. 1479–1493, 1992.

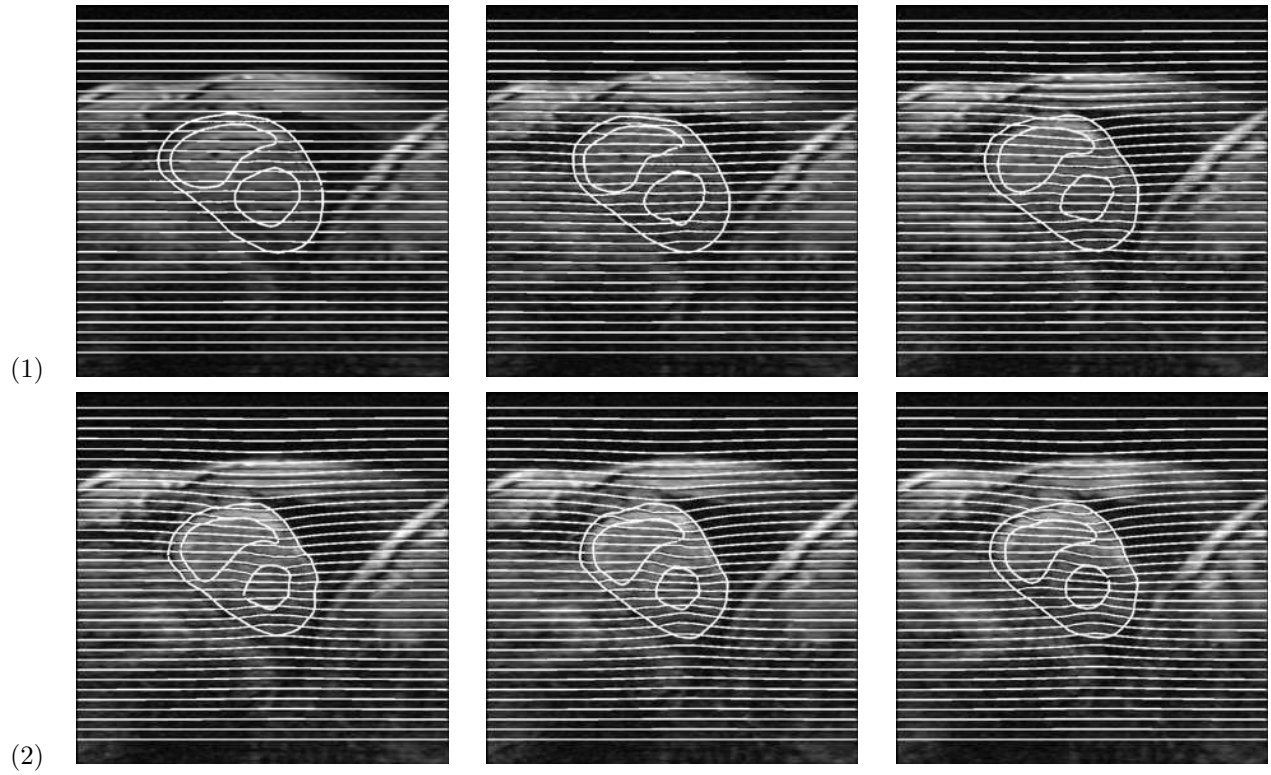

Figure 8. Contour and tag results generated by our system for a SA horizontal-tagged data set at position **7** at time 1, 3, 5, 7, 9, and 11.

12. J. Daugman, "Uncertainty relation for resolution in space, spatial frequency, and orientation optimized by two-dimensional visual cortical filters," *Journal of the Optical Society of America A* **2**(7), pp. 1160–1169, 1985.
13. Z. Qian, A. Montillo, D. Metaxas, and L. Axel, "Segmenting cardiac mri tagging lines using gabor filter banks," in *Proc of Int'l Conf. of the Engineering in Medicine and Biology Society*, pp. 630–633, 2003.